Journal of Metallurgy and Materials Science, Vol. 58, No. 4, October-December 2016, pp. 221-229
Printed in India, © NML, ISSN 0972-4257

Study on flow properties of rotor grade steel

M.I. MEHTA*, B.P. KASHYAP[1] and R.K.P. SINGH
Kalyani Centre for Technology and Innovation, Bharat Forge Ltd.
Pune-411 036, India
[1]IIT Bombay, Mumbai-400 076, India

Abstract : Compression tests were performed on Gleeble 3800 Thermo-Mechanical Simulator to study the flow properties of rotor grade steel 28CrMoNiV59. Compression specimens were deformed at a constant strain rate of 10^{-3} s^{-1}. The temperature range during tests was between room temperature and 1000°C with an interval of 100°C. When the normalized flow stress was plotted as a function of temperature, it exhibited three different regions. In regions I and III flow stress decreases with increase in temperature but the same increases with temperature in region II. Microstructural changes and work hardening behaviour have been studied for the deformed specimen. Furthermore, TEM analysis was also done for the samples of these three different regions (I, II & III). Strain hardening rate as a function of the normalized flow stresses decreases at larger strain and become negligible at higher temperature.

Keywords : Rotor grade steel, Flow properties, Gleeble 3800, Deformation.

INTRODUCTION

In power plants, turbine rotors are subjected to high temperatures especially during start up cycle. The rotor shaft is a spinning component, on which wheels and blades are attached. Initially steam is generated in a boiler which then hits the turbine blades at elevated temperature and pressure. The steam's impact causes the rotor to start spinning. This also causes sudden changes in the temperature and transient thermal stresses are induced in the turbine rotor. So, it becomes essential to estimate the thermal stresses induced in the turbine. Recently, C. Zhang et al.[1] has analysed the steam turbine for temperature variations and stresses generated in short period of time during the start and stop of cycle. Fig. 1 shows the temperature variation for 600MW supercritical steam turbine's rotor[1]. It is observed in Fig. 1 that the temperature variation in the rotor varies from 60°C to 542°C within 12000 sec from the start of the cycle. In order to understand the behaviour of the rotor shaft under the combination of the thermal as well as mechanical loads, it is important to understand the deformation behaviour of the material at different temperatures.

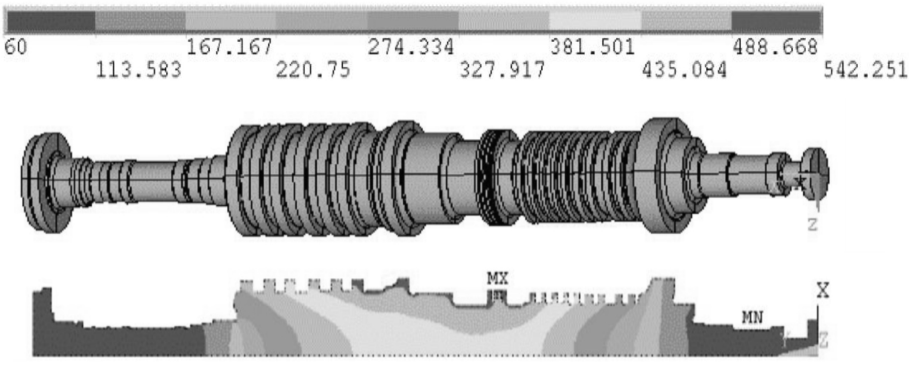

Fig. 1 : Temperature variation for 600MW supercritical turbine after 12000 sec[1]

**Corresponding Authors Email : mohan.mehta@bharatforge.com, bpk@iitb.ac.in, rajkumarsingh@bharatforge.com*

The material flow behaviour during hot deformation is complex; hardening and softening mechanisms are affected by temperature and strain rate[2-3]. In thermo-mechanical processes, material undergoes several metallurgical phenomena such as work hardening[4], dynamic recovery[5] and dynamic recrystallization[6]. The effects of these phenomena are often exhibited in the flow curves.

In the current paper, compressive deformation behaviour of rotor grade steel was studied. The test temperatures were varied up to 1000°C. Compression tests were carried out to find out flow stress of rotor shaft for a wide range of temperatures at a constant strain rate of 10^{-3} s^{-1}. The stress- strain values obtained from tests may be used as input to the FEM analysis of the part for optimization of the design.

EXPERIMENTAL

Material for experiment

In the present study, rotor grade steel (28CrMoNiV59) was selected for the experiment, as this material is used for manufacturing of steam turbine rotor shaft. Chemical analysis was carried out on the selected rotor material to confirm the grade and chemistry of the selected steel.

Material for experiment was extracted from finished rotor shaft. This rotor shaft was manufactured using a process flow which is shown in Fig. 2. The rotor shaft was forged from ingot on 4000T hydraulic press. After forging, post heat treatments were carried out on the shaft to achieve required mechanical properties.

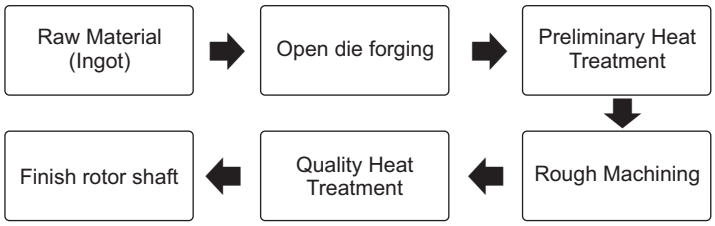

Fig. 2 : Flow chart of rotor shaft

The shaft was hardened by quenching from the austenizing temperature and later it was tempered in the temperature range of 690-750°C.The microstructure of as received heat treated material consists of ferrite and tempered martensite. Fig. 3 exhibits two different phases i.e. soft ferrite phase (bright) and hard martensite phase (dark). SEM image of the same is shown in Fig. 4. Prior austenitic grain boundaries can be observed in the SEM image.

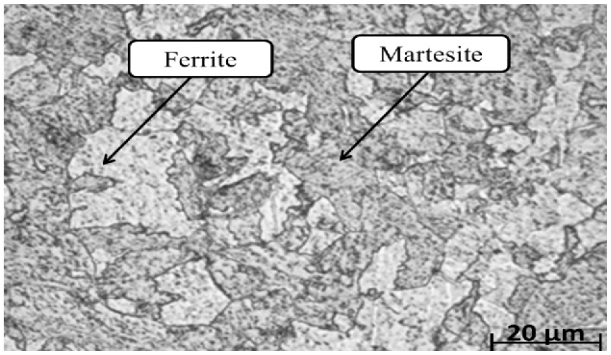

Fig. 3 : Optical image of heat treated steel sample when etched in nital 2%.(500X)

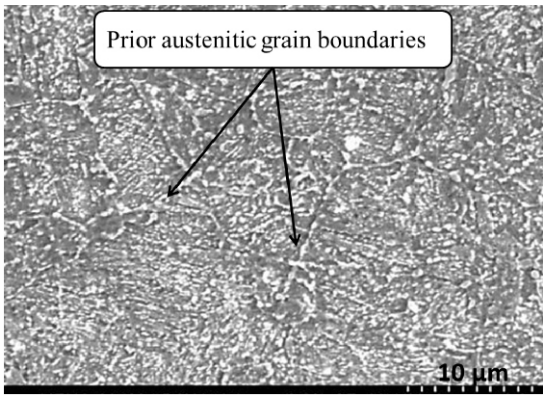

Fig. 4 : SEM image of heat treated sample

Mechanical testing

The mechanical properties of finished rotor shaft were determined by different tests like hardness test, tensile and impact test, at room temperature. Samples were taken out from rotor shaft for hardness testing. Furthermore, the oxide layers formed during heat treatment were removed by grinding. Hardness was measured using digital Rockwell hardness tester. Average value of three hardness readings at different positions was calculated. Indents were made on the polished surface using 150 kg load for HRc scale and 10 sec dwell time.

For tensile tests, cylindrical specimens were prepared as per ASTM E8 standard. Tensile testing was done on universal testing machine of make Zwick / Roell.

Impact specimens (extracted from rotor shaft) were prepared as per ASTM 23. The tests were conducted on Zwick/ Roell Charpy impact test machine. Three samples were tested and average value was calculated.

Compression testing

Flow properties of rotor grade steel (28CrMoNiV59) were determined by compression test. For compression testing, test specimens were prepared from rotor shaft in longitudinal direction by maintaining L/D ration of 1.5. The specimens for compression tests were cylindrical with diameter 10 mm and height 15 mm. Compression tests were performed by using a Gleeble 3800 thermo-mechanical simulator. Figure 5 shows schematic diagram of compression testing set up. ISO-T anvils were used for compression testing. A piece of 0.125 mm thick graphite foil was used as a lubricant in the uniaxial compression testing.

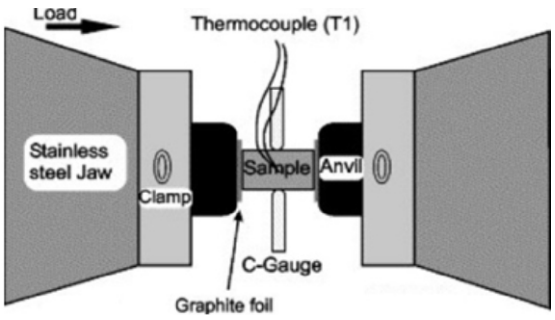

Fig. 5 : Schematic diagram of compression testing machine

Compression tests were performed with the constant strain rate of 10^{-3} s^{-1} from room temperature to 1000°C at an interval of 100°C. On each specimen, a K-type thermocouple was welded at the mid-span to control temperature during testing. Each specimen was heated with a heating rate of 5°C/s up to T-20°C where, T is the test temperature. In the temperature range from T-20°C to T, the heating rate was decreased to 2.5°C/s to prevent temperature overshooting. Once T was reached, 10 seconds of soaking time were given to stabilize the temperature in the sample. After the completion of test, each specimen was immediately subjected to rapid air cooling with the cooling rate of ~100°C/s to freeze the microstructure.

Test data have been recorded during testing. True strain and stress has been calculated from eq. 1 and eq. 2 respectively.

$$\varepsilon = \text{In}\left[\frac{h_o}{(h_o - \Delta h)}\right] \qquad \ldots (1)$$

where, h_o : Initial height of a specimen,

Δh : Cross-head displacement.

$$\sigma = \left[\frac{[F(h_o - \Delta h}{(S_o\, h_o)}\right] \qquad \ldots (2)$$

where, F : Measured load,

S_o : Initial cross sectional area.

Microstructure analysis

Microstructural analysis was carried out on compression test specimens. The optical micrographs were taken using bright field inverted stage microscope of Zeiss make. Scanning electron microscope (SEM) of Zeiss make was also used to examine specimen. For transmission electron microscopy, thin foils were prepared by thinning compression test specimen using emery paper. Final thinning was completed by jet electro polishing. Thin prepared foil was examined by transmission electron microscope of JEOL make (model-JEM1400) operating with an accelerating potential of 100kV.

RESULTS AND DISCUSSION

High strength and ductility are the critical properties for rotor grade steel. Microstructural analysis and deformation curves obtained from compression tests are discussed here.

Chemical analysis of the material

The result of the chemical analysis is given in the Table 1. It can be seen from the results that the values are well within spec.

Table 1: Chemical analysis results of 28CrMoNiV59

Alloying Elements	C	Mn	P	S	Si	Cr	Ni	Mo	V	Al
Obtained (wt%)	0.26	0.42	0.001	0.003	0.05	1.2	0.61	0.87	0.31	0.004

Mechanical test results

The results of tensile, impact and hardness tests, carried out at room temperature, are presented in Table 2.

Table 2 : Mechanical properties at room temperature

Yield Strength (Mpa)	Ultimate tensile Strength (Mpa)	% Elongation	Hardness (HRC)	Impact energy (J)
660	840	12.25	24	108

Compression test results

Compression specimens of rotor grade steel material were deformed up to 50% strain at a wide range of temperature from room temperature to 1000 °C at constant strain rate 10-3 s-1[7-8].

Figure 6 shows true stress-strain graphs of compression test at various conditions. Following can be observed from these graphs:

1. As the test temperature increases, stress required for deformation reduces.
2. The material exhibits almost same deformation behavior at temperatures 100, 200 and 300°C.

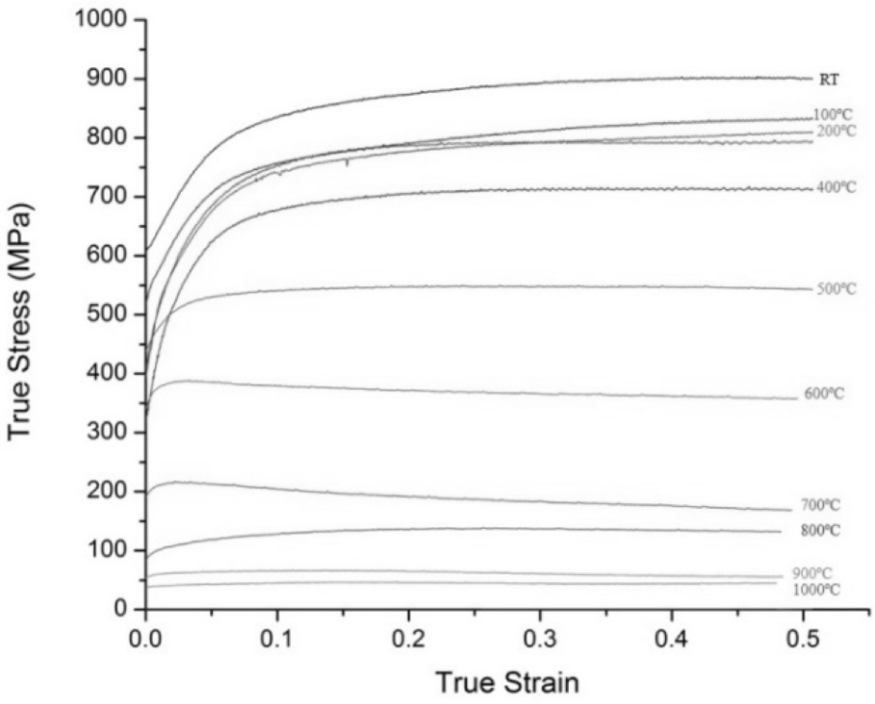

Fig. 6 : True stress strain curve over temperature ranges from room temperature to 1000°C at strain rate 10^{-3} s^{-1}.

The effect of temperature on stress at different strains is shown in in Fig. 7. Fig. 7 shows curves of σ/G vs. homologous temperature (T/Tm) which can be divided in to three different regions namely region I, II, and III as per the following observations:

1. The graph exhibits that in regions I and III, less flow stresses required as temperature increases.
2. In region II the slightly high flow stresses required.

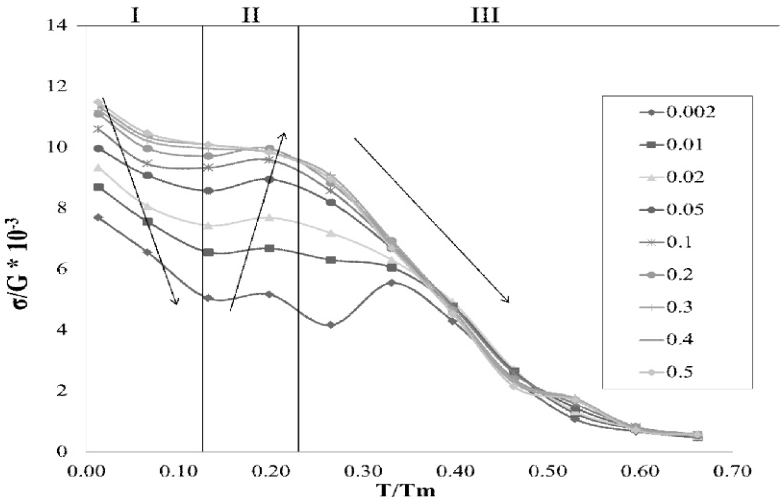

Fig. 7 : σ/E vs. Temperature (at ε = 0.002, 0.01, 0.02, 0.05, 0.1, 0.2, 0.3, 0.4, 0.5) at ε′ = 10^{-3} s^{-1}

The stresses required for deformation at lower temperatures (i.e. region I) are higher because the grain boundaries act as barrier to slip. In region III, diffusion plays a very important role which contributes to the decrease in stress with increasing temperature. In this temperature regime, diffusion helps in the movement of dislocation and thus, deformation becomes easier[9].

Microstructure analysis

The optical microstructure of specimens deformed at various temperatures was studied. No significant difference was observed in the microstructure of various deformed specimens as shown in Fig. 8. It shows that there is no effect of deformation and its temperature on the microstructure of the deformed specimen. But, it is seen that the deformation stresses increase

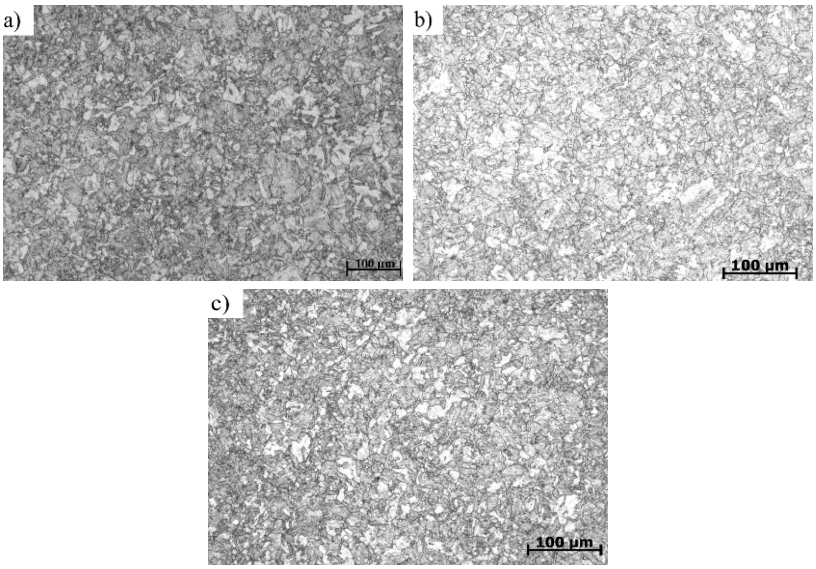

Fig 8 : Microstructure of the steel after hot compression at the temperature a) 100°C b) 300°C and c) 1000°C

with temperature in the region II. To find its root cause TEM analysis was carried out. In TEM analysis one specimen from each region was studied. TEM analysis results as shown in Fig. 9.

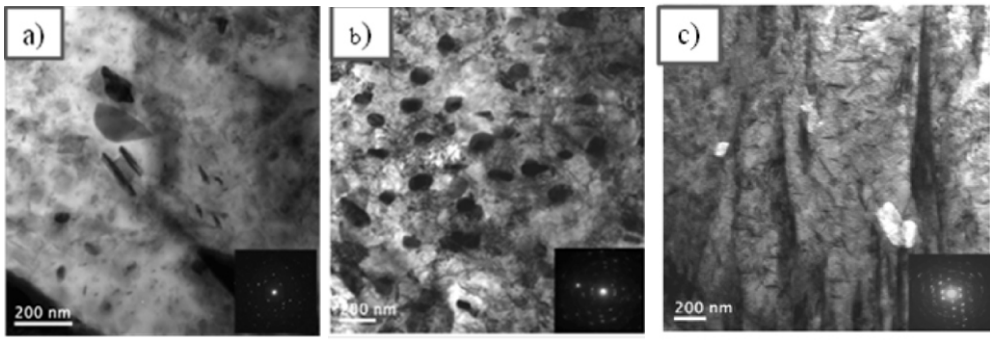

Fig. 9 : TEM micrographs of specimen compressed at a) region I room temperature b) region II 300°C and c) region III 1000°C

Following can be observed from the TEM results:

1. The region I and III samples shows less or negligible precipitates.
2. The region II samples show fine uniformly distributed precipitates.

Energy dispersive X-ray (EDX) technique was used to identify the composition of these precipitates in region II sample. Fig. 10 exhibits EDX spectra which show elements Cr, Fe. Hence, the formation of Cr carbide particle may be possible in the intermediate temperature range i.e. around 300°C. This may be the cause for barrier to the dislocation. Thus, increasing the flow stresses required for deformation in region II.

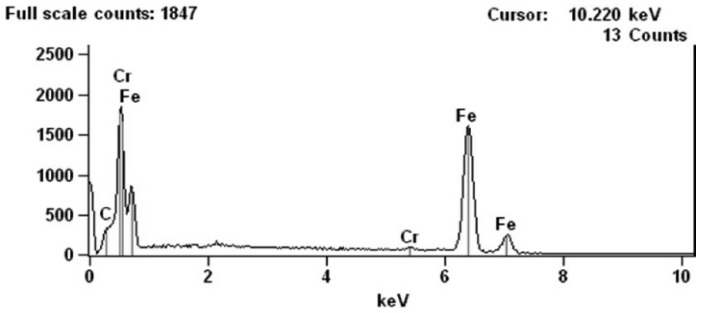

Fig. 10 : EDX spectra of compress sample at 300°C

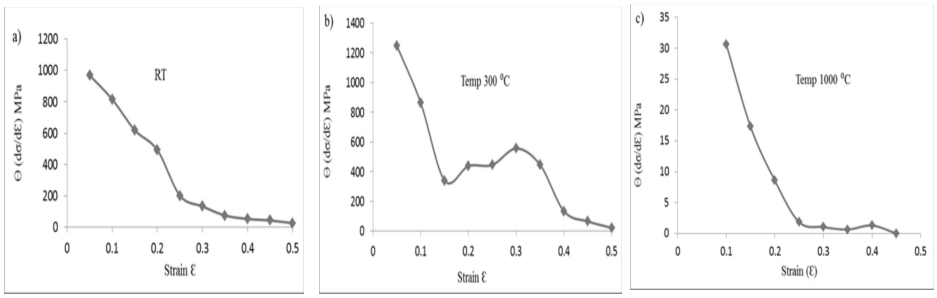

Fig. 11 : The variation in strain hardening rate ? as function of strain ? at a) room temp b) 300°C c) 1000°C

For understanding the compression flow behaviour, effect of strain hardening rate as a function of strain was studied. Fig. 11 (a), (b) and (c) shows variation in strain hardening rate for room temperature, 300°C and 1000°C respectively. These curves show variation with respect to strain. At low and high temperature, oil decreases almost linearly with increasing strain. But for intermediate temperature i.e. 300°C, increase is observed.

E. Isaac Samuel et al.[10] has used the variations of instantaneous work hardening rate ? as function of stress to study hardening behaviour. Similarly, for this study the strain hardening rate as a function of stress was plotted. The effect of strain hardening rate as function of normalized stress is as shown in Fig. 12. Compression test data obtained at all temperatures were analysed with respect and stress but only few representative plots are presented in Fig. 12. Low (room temperature), intermediate (300°C) and high (1000°C) temperature conditions are consider studying the variation. It can be observed that the strain hardening rate decreases with increase in strain and the same becomes negligible at higher temperature.

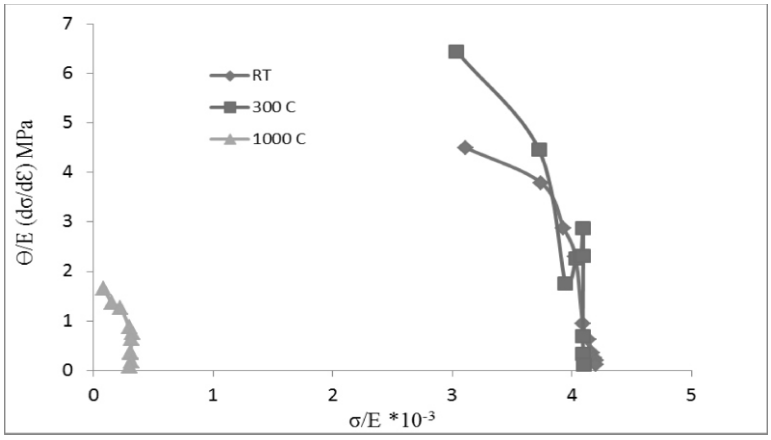

Fig. 12 : The variation in strain hardening rate as function of stress at a) room temp, b) 300°C, c) 1000 °C

CONCLUSIONS

- This investigation explored the effect of temperatures on flow properties of "28CrNiMoV59" during compression test. As the test temperature increases, stress required for deformation reduces.
- When the flow stress was plotted as a function of temperature, it exhibits three different regions. In regions I and III flow stress decreases with increase in temperature but the same increases with the temperature in region II.
- In region II, the increase in flow stress with temperature can be attributed to uniform precipitation of fine carbide particles which may cause barrier to dislocation (~200°C - 350°C).
- The strain hardening rate decreases with increase in strain. The same becomes negligible at higher temperature.

ACKNOWLEDGMENT

The authors would like to express a sense of gratitude towards Dr. Ilchat Sabirov (IMDEA Material Institute, Spain) and Dr. Devesh Mishra (Department of Chemical Engineering University of Louisiana at Lafayette, USA) for their sincere support.

The authors gratefully acknowledge the extended support provided to this work by KCTI (Kalyani Centre for Technology and Innovation) for providing financial funding, laboratory and library facilities. The authors also acknowledge the support provided by Bharat Forge Ltd, Pune and DSIR (Department of Scientific and Industrial Research), Govt. of India. Finally, the authors would like to express special thanks and gratitude to review committee and top management of Bharat Forge Ltd for granting the permission to publish/present the research work.

REFERENCES

[1] Zhang C., Hu N., Wang J., Qiping, Chen, Xiaoli F.He., (2010), IEEE 978-1-4244-4813-5/10/&25.00c.
[2] Dan W.J., Zhang W.G., Li S.H. and Lin Z.Q., (2007), Material Science and Engineering, **40**, pp. 101-107.
[3] Sommitsch C., Sievert R., Wlanis T., Gu¨nther B. and Wieser V., (2007), Material Science and Engineering, **39**, pp. 55-64.
[4] Imbert C.A.C. and McQueen H.J., (2001), Material Science and Engineering, A**313**, pp. 88-103.
[5] Roucoules C., Pietrzyk M. and Hodgson P.D., (2003), Material Science and Engineering, A **339**, pp. 1-9.
[6] Ponge D. and Gottstein G., (1998), Acta Materialia, **46**, pp. 69-80.
[7] Churyumov A.Yu., Khomutov M.G., Solonin A.N., Pozdniakov A.V. and Churyumova T.A., (2015), Materials and Design, **74**, pp. 44-54.
[8] Kashyap B.P., McTaggart K. and Tangri K., (1988), Philosophical Magazine, **57**(1), pp. 97-114.
[9] Callister W.D., (1940), Jr. Materials Science and Engineering, 7th Edn., John Wiley & Sons, USA, pp.109-112.
[10] Isaac Samuel E., Choudhary B.K. and Bhanu Sankara Rao K., (2002), Scripta Materialia, **46**, pp. 507-512.